S-Adenosyl-L-homocysteine hydrolase is sequestered into actin rods in *Dictyostelium discoideum* spores

Yoshiro Kishi[a], Teruko Sugo[b], Dana Mahadeo[c], David Cotter[c], Masazumi Sameshima[a,*]

[a] *Electron Microscopy Center, The Tokyo Metropolitan Institute of Medical Science, Tokyo Metropolitan Organization for Medical Research, 3-18-22 Honkomagome, Bunkyo-ku, Tokyo 113-8613, Japan*
[b] *Division of Cell and Molecular Medicine, Center for Molecular Medicine, Jichi Medical School, Yakushiji 3311-1, Tochigi 329-0498, Japan*
[c] *Department of Biological Sciences, University of Windsor, 401 Sunset Avenue, Windsor, ON, Canada N9B 3P4*

Received 16 October 2001; revised 24 October 2001; accepted 25 October 2001

First published online 6 November 2001

Edited by Jesus Avila

Abstract Here we show evidence that *S*-adenosyl-L-homocysteine hydrolase (SAHH) is linked to the actin cytoskeleton. Actin rods formed in *Dictyostelium discoideum* spores during the final stage of development are structurally composed of novel bundles of actin filaments. SAHH only accumulates with actin at this stage of development in the life cycle of *D. discoideum*. Recently SAHH is believed to be a target for antiviral chemotherapy and the suppression of T cells. Our finding may contribute to designing novel antiviral and immunosuppressive drugs.

Key words: *S*-Adenosyl-L-homocysteine hydrolase; Actin; Antivirus; *Dictyostelium*

1. Introduction

S-Adenosyl-L-homocysteine hydrolase (SAHH) plays a significant role in cellular methylation [1]. SAHH reversibly catalyzes *S*-adenosyl-homocysteine (SAH) into adenosine and L-homocysteine. An increase in the amount of SAH regulates the activity of methyltransferases that utilize *S*-adenosyl-L-methinine as a methyl donor. In fact, the treatment of cells with inhibitors of SAHH leads to deactivation of the SAH-dependent methyltransferases via SAH accumulation [2,3]. Methylation processes are also involved in viral replication and activation of T cells. Therefore SAHH is thought to be an attractive target for clinical applications such as antiviral chemotherapy and immunosuppressions [4–7]. On the other hand, there have been no reports on interaction between SAHH and the cytoskeleton.

The slime mold, *Dictyostelium discoideum*, is a primitive eukaryote that shows a well-defined developmental process upon depletion of food sources [8]. The amoebae migrate toward cAMP, which acts as a chemoattractant, and undergo multicellular development to form a fruiting body carrying a mass of spores into the air; the suspended mass of spores is known as the sorus [9]. The spores have large bundles of actin filaments called actin rods in both the nucleus and cytoplasm (Fig. 1A) [10,11]. The fine structure of the rod is quite novel (Fig. 1B). Electron microscopic images reveal that the actin rod is composed of hexagonally arranged tubules, which are believed to be constructed by three microfilaments [12]. This means that the rod may also contain novel factors such as actin-modulating proteins. In this study we investigated the components of the actin rods and found that SAHH accumulates in the actin rods in *D. discoideum* spores. This is the first report on a link between SAHH and the actin cytoskeleton.

2. Materials and methods

2.1. Cell culture, development and germination

Spores of *D. discoideum*, the wild type strain NC-4 and strain Ax2, were cultured on a nutrient agar plate with *Klebsiella aerogenes* or in a nutrient medium as previously described [13]. For synchronous development, growing cells freed from bacteria were starved for 4 h and spread on non-nutrient agar plates [13]. After 24 h fruiting bodies were formed, and spores at this time were designated as 0 day old spores. For inducing spore germination, washed spores were suspended in a nutrient germination medium containing 0.5% glucose, proteose peptone and 50 μg/ml partially purified SGPs at a density of 1×10^7 spores/ml [14]. Following the activation, spore suspensions were immediately transferred to a shaker at 22°C. The time when spore suspensions were transferred to the shaker was defined as 0 h. The live spores collected at the indicated times on the figures were observed under a ZEISS Axiophot fluorescent microscope using a $\times100$ plan objective lens. The presence of rod-like fluorescence of green fluorescent protein fused to SAHH (GFP-SAHH) in the nucleus or cytoplasm was determined by observing phase contrast images.

2.2. Reconstruction of actin rods in vitro

2-day-old spores were collected according to Kishi et al. [13] and homogenized by a cool mill (Tokken, Chiba, Japan) until more than 95% of the spores were broken. The homogenates were suspended in G-buffer (actin-depolymerizing buffer) containing 10 mM PIPES, pH 7.0, 3 mM EGTA, 0.2 mM DTT, 0.2 mM PMSF, 0.5 mM *ortho*-vanadate and a cocktail of protease inhibitors. After an ultracentrifugation at $400\,000\times g$ for 20 min at 4°C, a 1/10 volume of F-buffer (actin-polymerizing buffer) containing 500 mM PIPES, pH 7.0, 3 M KCl, 500 mM EGTA, 1 M $MgCl_2$ and 100 mM Na-ATP was added to the supernatant which was held at 25°C for 2 h. After an ultracentrifugation at $400\,000\times g$ for 20 min at 25°C, the pellet (P1) was suspended in G-buffer and dialyzed against this buffer at 4°C for 24 h to depolymerize precipitated actin. The resulting solution was centrifuged at $400\,000\times g$ for 20 min at 4°C, and a 1/10 volume of the F-buffer was added to the supernatant and kept for 2 h at 25°C. After an ultracentrifugation at $400\,000\times g$ for 20 min at 25°C, the pellet (P2) was suspended in G-buffer and dialyzed against this buffer at 4°C for 24 h to again depolymerize precipitated actin. This actin depolymerization and polymerization procedure was performed once more, and the final pellet (P3) was obtained. P1, P2 and P3 fraction were analyzed by transmission electron microscopy (TEM) and sodium dodecyl sulfate–polyacrylamide gel electrophoresis (SDS–PAGE) as described below.

*Corresponding author. Fax: (81)-3-3823 2965.
E-mail address: msameshi@rinshoken.or.jp (M. Sameshima).

0014-5793/01/$20.00
PII: S0014-5793(01)03105-2

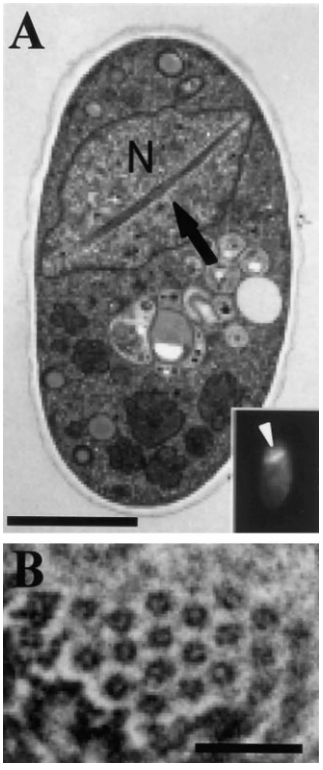

Fig. 1. TEM images of the *D. discoideum* spore. A: Arrow indicates an actin rod in the nucleus. Inset shows a fluorescent image of a spore stained with rhodamine-phalloidin, which specifically binds to actin filaments. Rod-like fluorescence is observed in the nucleus (arrowhead). Actin rods are also observed in the cytoplasm of spores (data not shown). N, nucleus. Bar, 3 μm. B: TEM image of a cross-section of actin tubules in the nuclear actin rod. Bar: 2 μm (A), 50 nm (B).

2.3. TEM

Spores and pellets were sandwiched between copper grids and quickly frozen by submersion in liquid propone using Leica WM CPC (Vienna, Austria). Specimens were freeze-substituted with absolute acetone containing 2% OsO_4 at −85°C for 3 days, warmed to −25°C, and transferred to ice [12]. Washed specimens with cold acetone were kept at room temperature for 30 min and then embedded in epoxy resin (Poly/Bed 812, Polyscience, Warrington, PA, USA). Spores were also fixed with 2.5% glutaraldehyde and then with 1.5% OsO_4 [10]. Ultrathin sections doubly stained with uranyl acetate and lead citrate were examined with a JEOL JEM-1200 EX TEM (JEOL, Tokyo, Japan). The diameter of microtubules was normalized to 25 nm.

2.4. Partial amino acid sequence analysis

Total proteins of spores and pellets were analyzed on SDS–PAGE according to Laemmli [15]. All the candidates of the components of actin rods were digested with lysylendopeptidase (E/S = 1/50, w/w) at 36°C for 16 h in 100 mM Tris–HCl, pH 9.0. The digests were injected onto a TSK-GEL ODS-80 TS column (4.6×150 mm), and the polypeptides were eluted with a linear gradient from 0 to 40% acetonitrile in 100 min (flow rate: 0.5 ml/min) according to Sugo et al. [16]. The polypeptides were subjected to the amino-terminal amino acid sequence analysis with a Protein Sequencer, model 476A (PE Biosystems, Foster City, CA, USA).

2.5. Vector

An expression vector for GFP-SAHH (pGFP-SAHH) was constructed as follows. Complementary DNA was amplified from RNA by polymerase chain reaction using two primers, SAHH-F (AAAAGTCGACATGACTAAATTACACTACAAAGTT) and SAHH-R (AAAACTCGAGTTAATATCTGTAGTGATCAACTTTGTATGG). Blunt ends were generated with the Klenow fragment and following digestion with *Sal*I, the cDNA was ligated into pHGFP [17], which had been treated sequentially with *Xho*I, Klenow fragment and *Sal*I to produce pGFP-SAHH. The plasmid was introduced into vegetative cells of strain Ax2 by electroporation and the transformed cells were selected in HL5 medium containing 7 μg/ml G418 [17].

3. Results and discussion

3.1. Reconstruction of actin rods in vitro

To analyze the components of actin rods in *D. discoideum* spores (Fig. 1), we first tried to isolate intact rods from spore homogenates. However the experiment failed because rods are sensitive to pressure [12]. Alternatively, we tried in vitro reconstruction of actin rods. Supernatants of spore homogenates were incubated under actin-polymerizing conditions. After the incubation, the pellets obtained by ultracentrifugation were quickly frozen and observed by TEM (Fig. 2A). Tubular structures approximately 13 nm in diameter, which is similar to that of the actin tubules of spore actin rods

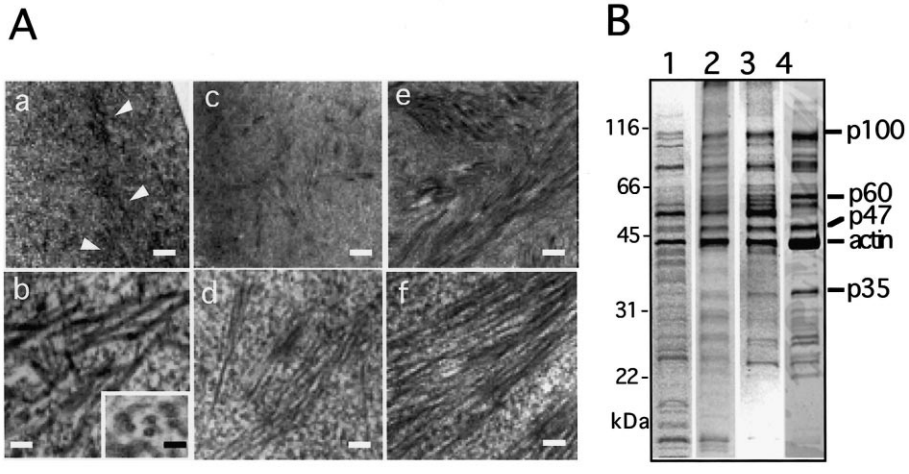

Fig. 2. Reconstruction of actin rods in vitro. A: a, c and e: TEM images of P1, P2 and P3 fractions, respectively. Arrowheads indicate thick filament 13 nm in diameter. b, d and f are enlarged images of a, c, and e, respectively. Inset in b shows the cross section of thick filaments. Bars in the upper column, 200 nm; bars in the lower column, 20 nm. B: Coomassie Brilliant Blue staining image after SDS–PAGE of each pellet. Lane 1: total proteins of spores. Lane 2: proteins of the pellet of a. Lane 3: proteins of the pellet of c. Lane 4: proteins of the pellet of e. Major proteins concentrated together with actin are named p100, p60, p47 and p35, corresponding to their molecular weights.

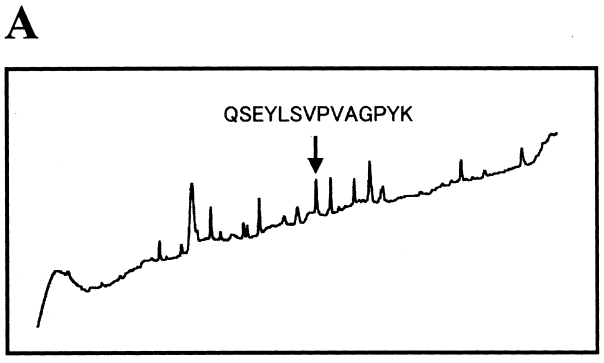

Fig. 3. p47 is *Dictyostelium* SAHH. A: HPLC profile of lysylendopeptidase digests of p47. One peak indicated by arrow was subjected to N-terminal amino acid sequence analysis. B: Amino acid sequence of *Dictyostelium* SAHH from a database: SWISS-PROT, P10819. The sequence data analyzed in A completely agreed with the underlined part of the amino acid sequence of *Dictyostelium* SAHH. The molecular weight of *Dictyostelium* SAHH is also 47 kDa.

(Fig. 1B), were observed in the pellet (Fig. 2A, a–b). Therefore actin tubules may be reconstructed from spore homogenates in vitro although they were loosely bundled as compared to intact rods in spores. To concentrate actin in the pellet, the pellet was dialyzed against the actin-depolymerizing buffer, and the supernatant after centrifugation was again incubated under actin-polymerizing conditions (Fig. 2A, c–d). This procedure was repeated once more. In the final pellet, actin filaments were heavily concentrated although tubular structures had not been observed (Fig. 2A, e–f). Coomassie Brilliant Blue staining images after SDS–PAGE of the pellets confirmed the accumulation of actin and showed many other polypeptides were concentrated during the reconstruction procedure (Fig. 2B). Major bands were named as p100, p60, p47 and p35, corresponding to their molecular weights (Fig. 2B, lane 4).

3.2. SAHH is a component of spore actin rods

Partial amino acid sequence analysis revealed that p47 is *Dictyostelium* SAHH (Fig. 3). After digestion of the p47 band with lysylendopeptidase, the polypeptides were separated by high performance liquid chromatography (HPLC) and the amino acid sequence in a peak was determined (Fig. 3A). The sequence, QSEYLSVPVAGPYK, perfectly agreed with that of *Dictyostelium* SAHH from 411 to 424 (Fig. 3B) [18,19]. Both molecular weights also agreed with each other.

To investigate whether SAHH associates onto actin rods in spores, we expressed GFP-SAHH in *D. discoideum* using an extra chromosomal expression vector [17]. Rod-like fluorescence was observed both in the nucleus and cytoplasm of the mature spores expressing GFP-SAHH using fluorescent microscopy (Fig. 4), while GFP-SAHH diffusely distributed in the cytoplasm and the nucleus of amoeboid cells (Fig. 6A,B). The rod-shaped fluorescence appeared during sporulation and disappeared during germination (Fig. 5). The time course and shape of the fluorescence of GFP-SAHH completely agreed with that of spore actin rods observed by TEM. Thus we conclude that SAHH interacts with the actin rods formed during the period of the dormant spore stages. In vitro, however, no actin tubules were observed in the final pellet (Fig. 2A, e–f). Therefore it seems that SAHH is in-

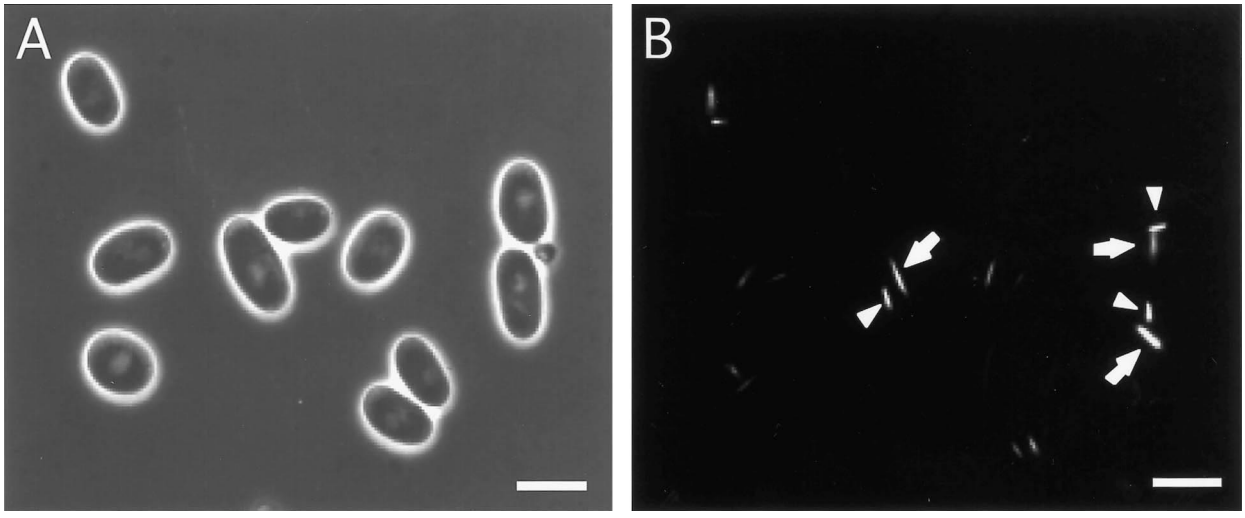

Fig. 4. Accumulation of GFP-SAHH on actin rods. Phase contrast image (A) and fluorescence image (B) of *D. discoideum* 2-day-old spores expressing GFP-SAHH. Bar, 10 μm. Rod-like fluorescence is observed both in the nucleus (arrowhead) and cytoplasm (arrow) of all spores.

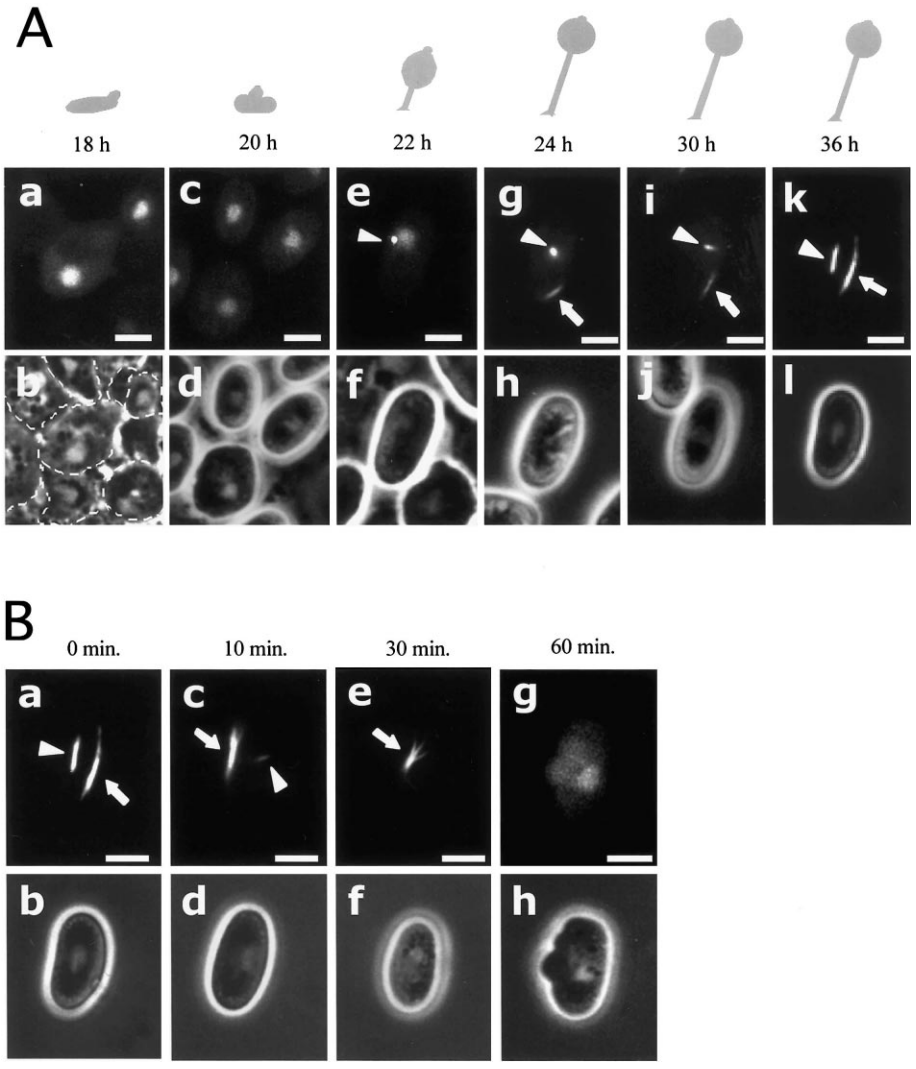

Fig. 5. Fluorescent images of GFP-SAHH in *D. discoideum* cells during sporulation (A) and germination (B). A: Illustrations represent the developmental process. Upper column shows fluorescent images, and lower column shows phase contrast images. Rod-shaped fluorescence appeared in the nucleus (arrowheads) and cytoplasm (arrow) after 22 h of development. Bar, 3μm. B: 2-day-old spores were stimulated with the germination medium (see Section 2) and maintained for the indicated minutes. Upper column, fluorescent images; lower column: phase contrast images. Rod-shaped fluorescence in the nucleus (arrowheads) and cytoplasm (arrow) disappeared during spore germination. Bar, 3 μm.

volved in bundling of tubules in vivo rather than the formation of actin tubules itself.

Partial amino acid sequence analyses also showed that p100, p60 and p35 were *Dictyostelium* cdc48, a homologue of pyrroline-5-carboxylate dehydrogenase, and a homologue of microtubule-associated protein MAP1B, respectively. The GFP-fused constructs of these proteins did not localize to the actin rods of *Dictyostelium* spores in vivo (data not shown).

3.3. SAHH, actin rods, and actin tyrosine phosphorylation

Physiologically, spores of *Dictyostelium* are static. The oxygen consumption of spores is 10-fold less than that of amoebae, and the rate of glycolysis and many synthetic reactions are low. This fact and sequestering of SAHH into actin rods indicate that activity of SAHH may be restricted to a significant low level in the spores, although there is no information concerning cellular methylation in *Dictyostelium* spores. We believe that understanding the mechanism of the interaction between SAHH and the actin rod may give an attractive cue to the creation of new inhibitors of SAH-dependent methyltransferases, which also could be a new strategy for antiviral and immunosuppressive drug therapies. Concerning this point, we show that tyrosine phosphorylation of actin may be involved in the interaction of SAHH with the actin cytoskeleton. In *Dictyostelium* spores, half of actin molecules are in the tyrosine-phosphorylated form, and a decline of the phosphorylation levels is a prerequisite for spore germination [13,14]. Although the tyrosine phosphorylation levels of actin in amoebae are very low, treatment of the amoebae with oxidative depletion, dinitrophenol, azide and phenylarsine oxide (PAO), a specific inhibitor of protein tyrosine phosphatases, induces a significant increase in the phosphorylation levels of actin [20,21]. Interestingly, rod or dot-like fluorescence of GFP-SAHH appeared in the nucleus and cytoplasm of the amoebae treated with DNP, azide and PAO (Fig. 6). Additionally the phosphorylation site of actin is Tyr-53 in both the amoebae and spores (unpublished observations) [22]. Thus, SAHH accumulation into actin cytoskeleton may correlate

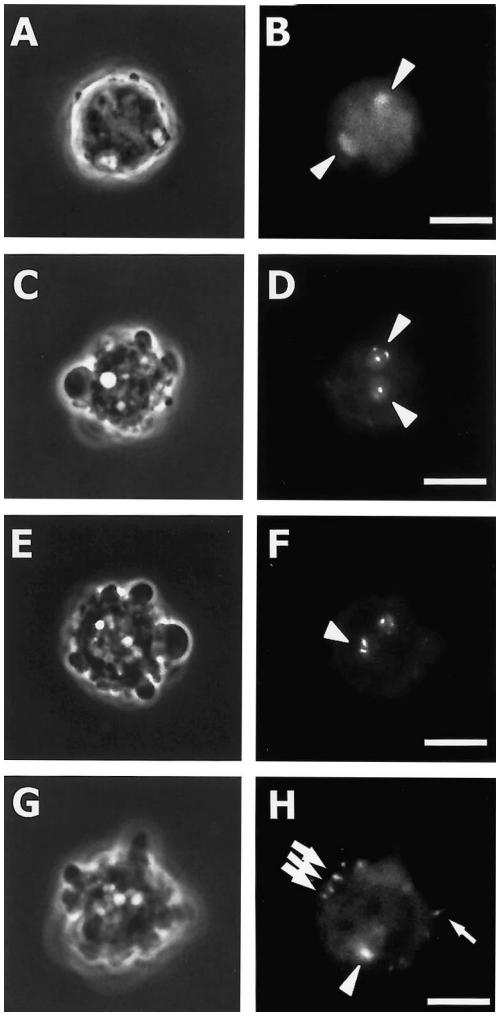

Fig. 6. Fluorescent images of GFP-SAHH in *D. discoideum* amoebae treated with inhibitors of ATP synthesis and protein tyrosine phosphatases. Left column: phase contrast images, right column: fluorescent images. Control cells (A–B). Amoebae cells were cultured in a nutrient medium containing 1 mM DNP (C–D), 1 mM azide (E–F), and 30 μM PAO (G–H) for 10 min. Rod or dot-shaped fluorescence appeared in the nucleus (arrowheads) and cytoplasm (arrow). Bar, 5μm.

with tyrosine phosphorylation of actin molecules. Whether SAHH directly binds to tyrosine-phosphorylated actin is now under investigation.

Acknowledgements: We thank Ms. Chizuko Nakamikawa and Dr. Hiroyuki Aizawa for helpful technical supports and the generous gift of a vector encoding pHGFP. We are also grateful to Dr. Ichiro Yahara for encouragement and support of this work. This work was supported by a Research Aid of the Inoue Foundation for Science to Y.K.

References

[1] Mann, J.D. and Mudol, S.H. (1963) J. Biol. Chem. 238, 381–385.
[2] Wnuk, S.F., Mao, Y., Yuan, C.S., Borchardt, R.T., Andrei, G., Balzarini, J., De Clercq, E. and Robins, M.J. (1998) J. Med. Chem. 41, 3078–3083.
[3] Muzard, M., Vandenplas, C., Guillerm, D. and Guillerm, G. (1998) J. Enzym. Inhib. 13, 443–456.
[4] Bray, M., Driscoll, J. and Huggins, J.W. (2000) Antiviral Res. 45, 135–147.
[5] Saso, Y., Conner, E.M., Teegarden, B.R. and Yuan, C.S. (2001) J. Pharm. Exp. Ther. 296, 106–112.
[6] Wolos, J.A., Frondorf, K.A. and Esser, R.E. (1993) J. Immunol. 151, 526–534.
[7] Wolos, J.A., Frondorf, K.A., Davis, G.F., Jarvi, E.T., McCarthy, J.R. and Bowlin, T.L. (1993) J. Immunol. 150, 3264–3273.
[8] Cotter, D.A., Sands, T.W., Virdy, K.J., North, M.J., Klein, G. and Satre, M. (1992) Biochem. Cell Biol. 70, 892–919.
[9] Sameshima, M. (1993) Cytologia 58, 361–366.
[10] Sameshima, M., Chijiiwa, Y., Kishi, Y. and Hashimoto, Y. (1994) Cell Struct. Funct. 19, 189–194.
[11] Kishi, Y., Chijiiwa, Y., Sameshima, M. and Hashimoto, Y. (1994) Cytologia 59, 453–460.
[12] Sameshima, M., Kishi, Y., Osumi, M., Mahadeo, D. and Cotter, D. (2000) Cell Struct. Funct. 25, 291–295.
[13] Kishi, Y., Clements, C., Mahadeo, D., Cotter, D.A. and Sameshima, M. (1998) J. Cell Sci. 111, 2923–2932.
[14] Kishi, Y., Mahadeo, D., Cervi, D., Clements, C., Cotter, D.A. and Sameshima, M. (2000) Exp. Cell Res. 261, 187–198.
[15] Laemmli, U.K. (1970) Nature 227, 680–685.
[16] Sugo, T., Nakamikawa, C., Yoshida, N., Niwa, K., Sameshima, M., Mimuro, J., Weisel, J.W., Nagiata, A. and Matsuda, M. (2000) Blood 96, 3779–3785.
[17] Aizawa, H., Fukui, Y. and Yahara, I. (1997) J. Cell Sci. 110, 2333–2344.
[18] Guitton, M.C., Part, D. and Veron, M. (1988) Biochimie 70, 835–840.
[19] Kasir, J., Aksamit, R.R., Backlund, P.S. and Cantoni, G.L. (1988) Biochem. Biophys. Res. Commun. 153, 359–364.
[20] Schweiger, A., Mihalache, O., Ecke, M. and Gerisch, G. (1992) J. Cell Sci. 102, 601–609.
[21] Jungbluth, A., von Arnim, V., Biegelmann, E., Humbel, B., Schweiger, A. and Gerisch, G. (1994) J. Cell Sci. 107, 117–125.
[22] Jungbluth, A., Eckerskorn, C., Gerisch, G., Lottspeich, F., Stocker, S. and Schweiger, A. (1995) FEBS Lett. 375, 87–90.